Terahertz wide aperture reflection tomography

Jeremy Pearce, Hyeokho Choi, and Daniel M. Mittleman

Department of Electrical and Computer Engineering, MS 366, Rice University, Houston, Texas 77251-1892

Jeff White and David Zimdars

Picometrix, Inc., 2925 Boardwalk, Ann Arbor, Michigan 48104-6765

We describe a powerful imaging modality for terahertz (THz) radiation, THz wide aperture reflection tomography (WART). Edge maps of an object's cross section are reconstructed from a series of time-domain reflection measurements at different viewing angles. Each measurement corresponds to a parallel line projection of the object's cross section. The filtered backprojection algorithm is applied to recover the image from the projection data. To our knowledge, this is the first demonstration of a reflection computed tomography technique using electromagnetic waves. We demonstrate the capabilities of THz WART by imaging the cross sections of two test objects. © 2005 Optical Society of America

OCIS codes: 110.6960, 320.7100.

For many imaging applications using terahertz (THz) radiation, it is desirable to work in a reflection mode, especially in situations when only one side of the object is accessible to detectors or when the object is opaque. We describe a powerful reflection imaging modality, THz wide aperture reflection tomography (WART), which can form high-resolution images of an object's cross section. In THz WART, an object is illuminated with a THz beam at a set of different viewing angles, and the backreflected waves are measured using a THz transceiver. The measured reflections correspond to parallel projections through the cross section, and therefore such computed tomography (CT) reconstruction algorithms as the filtered backprojection (FBP) algorithm can be applied to retrieve an edge map of the object's cross section. To our knowledge, THz WART is the first CT system for electromagnetic waves at any frequency that works in reflection mode, although similar methods have been explored using ultrasonic techniques.[1]

The use of THz time-domain spectroscopy for imaging in a reflection mode was first demonstrated in 1997.[2,3] Here, the refractive-index profile of the object was estimated by direct application of the Fresnel coefficients to the time-domain waveforms. However, these measurements were limited to a single viewing angle, which prevented the detection of objects located behind strong reflectors. Ferguson *et al.* subsequently used THz pulses in a transmission CT modality that is analogous to x-ray CT.[4] From measurements at several viewing angles, both absorption images and refractive-index images could be obtained. This technique requires a large number of measurements and is applicable only to transparent objects. Other techniques that have been studied include synthetic aperture radar,[5] time reversal imaging,[6,7] multistatic reflection imaging,[8] and synthetic phased-array techniques.[9,10] In each case, THz images have been reconstructed from reflection measurements obtained at multiple viewing angles. These techniques are limited by the need for a large number of measurements or by the resolution of the

image. In all cases, the optical system consists of a separate transmitter and receiver, which complicate the optical alignment.

The WART imaging system consists of a THz transceiver[11] in which both transmission and detection are accomplished via ultrafast photoconductive sampling,[12] a cylindrical lens, and a rotation stage as illustrated in Fig. 1. The transceiver emits single-cycle pulses of THz radiation into free space. We calculate the coherence length of the incident pulse to be $L_C \sim 820 \ \mu$m from the $1/e$ full width of the power spectrum.[13] In the present situation, where we directly measure the THz electric field in a reflection geometry, we expect that the range resolution should be somewhat smaller than $0.5 \ L_C$. This radiation is focused to a horizontal line using a cylindrical lens (focal length 12 cm) to restrict the illumination of the object to a thin horizontal slice as illustrated by the dashed lines in Fig. 1. The focal spot of the cylindrical lens controls the thickness of the illuminated slice, which therefore governs the ability to distinguish features in the vertical direction. The size of the illumination spot is less than 5 mm in the vertical direction and approximately 30 mm in the horizontal direction. The object is rotated in 1° increments over 360°, which allows the transceiver to obtain a com-
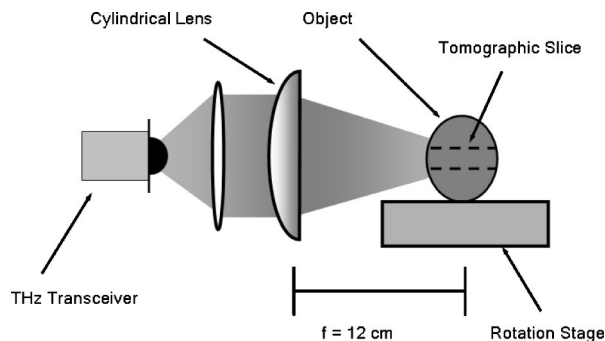

Fig. 1. THz WART setup. A THz transceiver illuminates a thin cross section of the object and measures the backreflected waves.

plete view of the tomographic slice. For each rotation increment, a THz waveform is acquired, spanning a 400 ps time window, at a rate of 50 ps/s.

For a given viewing angle, the temporal waveform consists of specular backreflections from forward-facing edges within the tomographic slice. The backward-facing edges are captured in the 180° complement measurement. Because the incident radiation is a plane wave, each reflection from the different portions of the object that lie on the same phase front will coherently sum, weighted by its reflectivity. It is appropriate to consider each measured waveform as a convolution of the parallel projection of the object's two-dimensional reflectivity edge map with the incident pulse. The measured time-domain reflected waveform $s(\theta,t)$ for viewing angle θ can be written as

$$s(\theta,t) = \int r(t - 2u/c) \, p_\theta(u) \mathrm{d}u, \tag{1}$$

where $r(t)$ is the incident pulse, $p_\theta(u)$ is the projection of the object slice, u is a point on the projection axis, and c is the speed of light within the slice. The projections $p_\theta(u)$ are related to the reflectivity edge map $f(x,y)$ by the Radon transform[4,14]:

$$p_\theta(u) = \int_{-\infty}^{\infty} \int_{-\infty}^{\infty} f(u \cos \theta - s \sin \theta, u \sin \theta + s \cos \theta) \mathrm{d}s. \tag{2}$$

Equation (1) is the convolution of the object's parallel projection with the incident pulse. To reconstruct an image of the tomographic slice, we first deconvolve $p_\theta(u)$ from $s(\theta,t)$ and then apply the FBP algorithm to recover the image. We use a hybrid Fourier-wavelet regularized deconvolution algorithm to retrieve $p_\theta(u)$ from $s(\theta,t),$[15] because it minimizes the artifacts that are associated with pure Fourier-based approaches. The FBP algorithm is based on the Fourier slice theorem, which relates the Fourier transform of an image projection to a slice in the two-dimensional Fourier transform of the image. The FBP algorithm inverts Eq. (2) to recover $f(x,y)$ by first filtering the projection data with a ramp filter and then backprojecting it across the image plane.[14] An image is reconstructed by summing all the resulting backprojections.

We demonstrate the imaging technique using two metal test objects as shown in Fig. 2. Because metals are highly reflective, a transmission geometry cannot be used to image these objects. In both cases, the object is translationally invariant in the dimension perpendicular to the image. For more complicated objects, the sample could be imaged at multiple heights to generate a full three-dimensional image.

Using the FBP procedure, we reconstruct images of the test objects from the full 360° range of viewing angles. The reconstructed images, shown in Figs. 2(a) and 2(c), capture most of the details of the outside edges, including in particular the small indentations around the border of the square object [see the photo in Fig. 2(d)]. The depth of these features is approxi-

mately equal to half of the coherence length of the THz radiation. Figure 2(b) shows a slice through the center of the image of Fig. 2(a), demonstrating the bandwidth-limited location of the object's edges.

As with any tomographic imaging technique, the quality of these images depends on the size of the data set. As fewer waveforms are used in the construction, the image quality degrades (see Fig. 3). This degradation can be quantified by correlating these incomplete reconstructions with an ideal image of the target, which would be obtained with an infinite data set (i.e., a continuum of projections). We can construct an approximate version of the ideal image by applying a threshold filter to our highest-quality reconstruction [Figs. 2(a) and 2(c)]. This estimate is then correlated with each reconstruction using a subset of the data, corresponding to a number of equally spaced viewing angles. Figure 4 plots the resulting correlation coefficient as a function of the number of
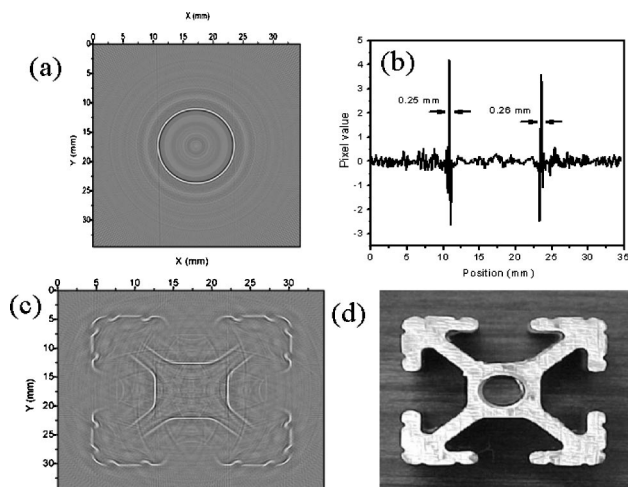

Fig. 2. (a) WART image of a cylindrical metal post. (b) Slice through the center of the image in (a), showing bandwidth-limited resolution of the surface. (c) WART image of a more complex metal object, with surface features of size comparable to half of the coherence length. (d) Photograph of the test object imaged in (c).
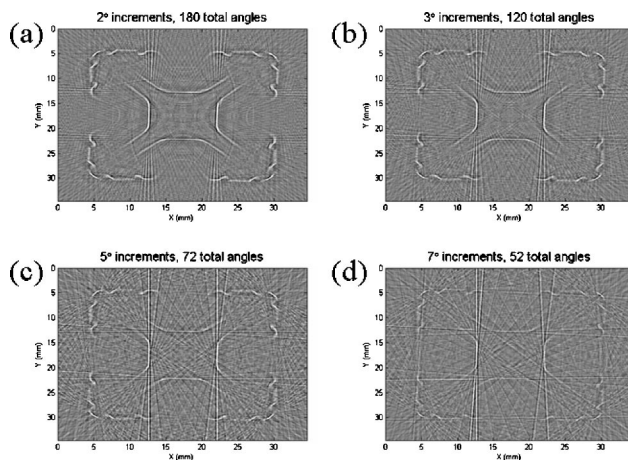

Fig. 3. THz WART images of the object shown in Fig. 2(c), reconstructed with subsets of the full data set. These images use (a) 180, (b) 120, (c) 72, and (d) 52 waveforms.
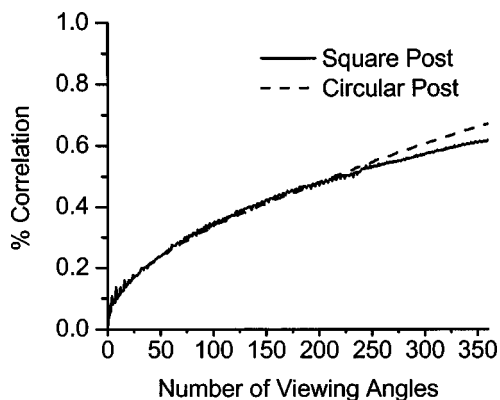
Fig. 4. Correlation of an ideal image, formed by applying a binary threshold to the highest-quality image, with each reconstruction formed using subsets of the full data set. The solid curve is the result for the corrugated post [Fig. 2(c)], while the dashed curve shows the result for the circular post [Fig. 2(a)]. As the number of waveforms used for image reconstruction decreases, the correlation between the resulting image and the ideal image decreases.

views used in the reconstruction, for both test objects. The similarity of these two results suggests that the size of the data set required for a given image quality does not depend on the shape or complexity of the object.

In conclusion, we have developed what is believed to be the first CT imaging system using electromagnetic waves in reflection mode. THz WART successfully recovered high-quality high-resolution images of two test objects. Features smaller than 0.5 mm in size were resolved using this tomographic reconstruction. THz WART can be extended to three dimensions by capturing images in successive elevations, similar to a traditional x-ray CT scan.[4] This technique can also be applied to transparent dielectric targets. However, large variations in phase velocity will lead to significant refraction, which will distort the otherwise flat phase fronts required for a coherent summation of backprojections. Additional work is required to extend THz WART to encompass objects with inhomogeneous velocity profiles.

References

1. K. A. Dines and S. A. Goss, IEEE Trans. Ultrason. Ferroelectr. Freq. Control **UFFC-34**, 309 (1987).
2. D. M. Mittleman, S. Hunsche, L. Bovin, and M. C. Nuss, Opt. Lett. **22**, 904 (1997).
3. D. M. Mittleman, M. Gupta, R. Neelamani, R. G. Baraniuk, J. V. Rudd, and M. Koch, Appl. Phys. B **68**, 1085 (1999).
4. B. Ferguson, S. Wang, D. Gray, D. Abbot, and X.-C. Zhang, Opt. Lett. **27**, 1312 (2002).
5. K. McClatchey, M. T. Reiten, and R. A. Cheville, Appl. Phys. Lett. **79**, 4485 (2001).
6. A. B. Ruffin, J. V. Rudd, J. Decker, L. Sanchez-Palencia, L. L. Hor, J. F. Whitacker, and T. B. Norris, IEEE J. Quantum Electron. **38**, 1110 (2002).
7. T. Buma and T. B. Norris, Appl. Phys. Lett. **84**, 2196 (2004).
8. T. D. Dorney, W. W. Symes, R. G. Baraniuk, and D. M. Mittleman, J. Opt. Soc. Am. A **19**, 1432 (2002).
9. J. O'Hara and D. Grischkowsky, Opt. Lett. **27**, 1070 (2002).
10. J. O'Hara and D. Grischkowsky, J. Opt. Soc. Am. B **21**, 1178 (2004).
11. M. Tani, Z. Jiang, and X.-C. Zhang, Electron. Lett. **36**, 804 (2000).
12. P. R. Smith, D. H. Auston, and M. C. Nuss, IEEE J. Quantum Electron. **24**, 255 (1988).
13. J. L. Johnson, T. D. Dorney, and D. M. Mittleman, IEEE J. Sel. Top. Quantum Electron. **7**, 592 (2001).
14. A. C. Kak and M. Slaney, *Principles of Computerized Tomographic Imaging* (IEEE Press, 1988).
15. R. Neelamani, H. Choi, and R. Baranuik, IEEE Trans. Signal Process. **52**, 418 (2004).